ChemComm

Accepted Manuscript

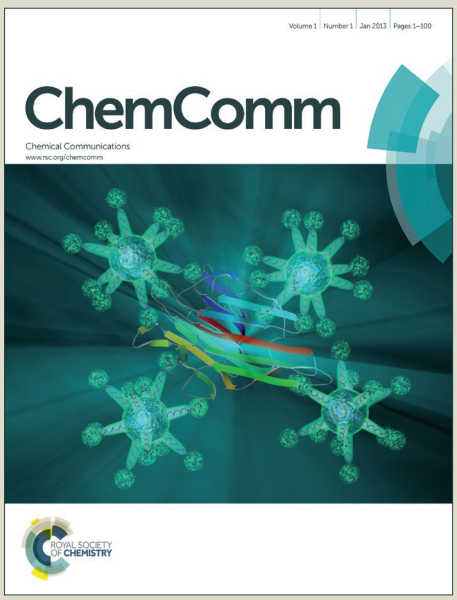

ROYAL SOCIETY OF CHEMISTRY

www.rsc.org/chemcomm

Journal Name

RSCPublishing

COMMUNICATION

Carbon Monoxide Mediated Chemical Deposition of Pt or Pd Quasi-Monolayer on Au Surfaces with Superior Electrocatalysis of Ethanol Oxidation in Alkaline Media

Cite this: DOI: 10.1039/x0xx00000x

Han Wang[†], Kun Jiang[†], Qiao-Li Chen[‡], Zhao-Xiong Xie[‡] and Wen-Bin Cai[†]*

Received 00th January 2012,
Accepted 00th January 2012

DOI: 10.1039/x0xx00000x

www.rsc.org/

Electroless deposition of a quasi-monolayer (q-ML) of Pt and/or Pd on different Au substrates is achieved by using CO as both reducing and quenching agents, imparting Au@Pt/C or Au@Pd/C with superior electrocatalytic activity for ethanol oxidation in alkaline media.

Platinum group metals (PGMs) like Pt and Pd are important catalytic metals used to drive numerous heterogeneous reactions including those involved in low-temperature fuel cells.[1] However, PGMs restrain their large scale application owing to not only high cost but also rare reserve.[2] To tackle this bottleneck, one of the ideal solutions is the construction of a (sub)monolayer (ML) of PGM on non-PGM metal substrate, to maximize the utilization of PGMs in heterogeneous reactions[3-7] as well as to take advantage of the synergistic effect due to the interaction between the PGM overlayer and non-PGM substrates. Specifically, Pt (sub)monolayer deposited on Au[5-10] was proved to promote electrocatalytic reactions including but not limited to methanol/ethanol oxidation,[5-7] oxygen reduction[8] and formic acid oxidation[9, 10].

There are two widely accepted wet-process strategies to grow Pt or Pd overlayers on Au, one is chemical (or electroless) deposition, and the other involves electrochemical deposition. Chemical deposition of a Pt or Pd overlayers of varying mass-equivalent thicknesses on Au colloids was achieved from Pt(II) or Pd(II) containing–precursors using L-ascorbic acid as the reductant.[11, 12] Recently, spontaneous deposition of Pt overlayers on Au nanoparticles from a temperature-raised Pt(II)-containing bath was reported for catalyzing ORR,[13] but the Pt deposit structure may not be well controlled. It should be pointed out that the deposition of a Pt (sub)monolayer on Au is not trivial, since Pt tends to grow in the form of 3D clusters on Au,[14] compromising the Pt mass utilization. So far, the controlled 2D deposition of Pt-ML on Au is overwhelmingly limited to external potential control. A well-known two-step process in which a Cu-ML is under-potentially deposited (UPD) on Au followed by subsequent galvanic redox replacement of Cu with Pt in a Pt(II)-containing solution.[15, 16] This process should be given with care to avoid the trapping of partial Cu.[3] A direct electrodeposition of a Pt ML on Au was reported by applying a very negative potential to the Au electrode in a selected plating bath[3] and using the strongly adsorbed H to block the further growth of Pt atoms. Alternatively, the electro-deposition of a Pt-ML on a polycrystalline Au film electrode was accomplished in a CO-saturated Pt(II) precursor solution under a flow cell condition.[4] The validity of the latter was later supported by STM observation on Au(111).[17] Unfortunately, unlike chemical deposition, the electrodeposition protocol is inconvenient or even unfavourable for a scale-up synthesis or modification of Au@PGM-based catalysts, especially in the case of highly dispersed Au nanoparticles.

To address this concern, we report herewith a facile chemical deposition of a quasi-monolayer (q-ML) of Pt and/ or Pd on different Au substrates at room-temperature, in which CO in the precursor solution serves as both reducing and quenching agents without external potential control. Attenuated total reflection-surface enhanced infrared adsorption spectroscopy (ATR-SEIRAS), X-ray diffraction (XRD), transmission electron microscopy (TEM)-energy dispersive spectroscopy (EDS) and cyclic voltammetry were applied to characterize the Pt or Pd overlayer structure. As a preliminary and important application in electrocatalysis, the as-formed carbon supported Au@PGM catalysts were examined for ethanol oxidation reaction (EOR) in alkaline media, demonstrating extraordinarily high activity.

Briefly, electroless deposition of a q-ML of PGM on Au surfaces was carried out by immersing polycrystalline Au (bulk or film) electrode or dispersing commercial Au/C (Au: ~5nm, 30 wt. %, TKK) in a CO-saturated 0.1 mM K_2PtCl_4 and/or Na_2PdCl_4 with a Au/PGM atomic fraction of 1/0.4 under ultrasonication for 10 min at room temperature. The as-formed Au/PGM electrode was emerged and rinsed with ultrapure Mill-Q water and served as the working electrode in the spectroelectrochemical measurement. For comparison, a 10-nm-thick Pt overlayer was electrodeposited on Au, denoted as Au/Pt-10 nm. Au@PGM/C nanoparticles were collected

and rinsed by centrifugation and then dried in vacuum oven at 60 °C. These catalysts were suspended in mixed water and Nafion solution under ultrasonication which was then casted on a glassy carbon electrode for electrocatalytic evaluation (see ESI for details). A possible growth mechanism of a PGM q-ML on Au is depicted in Fig. S1 and Scheme S1, involving the carbonyl complex formation in the CO-saturated Pt(II) or Pd(II) precursor, and its preferential decomposition on Au surfaces due to strong Au-PGM interaction to grow Pt or Pd adatoms, followed by strong CO adsorption to signicantly quench further growth of Pt or Pd into 3D clusters. Notably, "quasi-monolayer" instead of "monolayer" used in this paper is meant to assume the imperfection of the monolayer formed.

Fig. 1A shows the cyclic voltammograms (CVs) of polycrystalline Au, Au/Pt and Au/Pt-10 nm bulk electrodes in 0.5 M $HClO_4$. For the bare Au electrode, 0-1.3 V is essentially the double-layer potential region; CV for the Au/Pt electrode is very close to that for the electrochemically formed Au/Pt-ML electrodes (Fig. S2), with less hydrogen adsorption-desorption voltammetric feature emerges from 0 to 0.4 V. In contrast, the Au/Pt-10 nm electrode exhibited voltammetric features typical of a polycrystalline Pt electrode with notably increased surface area, due to the 3D growth and the absence of lattice and electronic effects of underlying Au on outermost Pt.

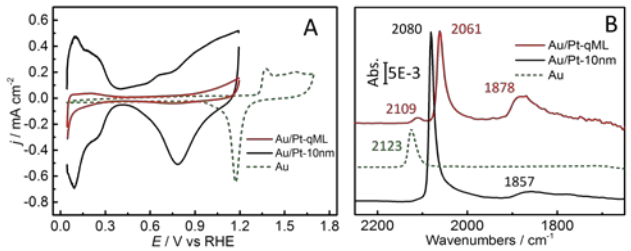

Fig. 1 (A) CVs of the Au/Pt, Au/Pt-10nm and Au bulk electrodes in 0.5 M $HClO_4$ solution. Scan rate: 50 mV s^{-1}. (B) ATR-SEIRAS spectra of adsorbed CO on Au/Pt, Au/Pt-10nm and Au film electrodes in a CO saturated 0.5 M $HClO_4$ solution at 0.31 V vs RHE.

The atomic ratio of Au to Pt (Pd) for Au@Pt, Au@Pd/C and Au@(Pt+Pd) was determined by ICP-AES to be ca. 1/0.32±0.05, more or less close to the value estimated by assuming a cuboctahedron model for 5-nm Au nanoparticles covered with a monolayer of PGM.[18] The surface structure of the Au/Pt film was characterized by ATR-SEIRAS measurement with CO being the surface probe, see Fig. 1B. In a CO-saturated 0.5 M $HClO_4$, the minor 2109-cm^{-1} band intensity for the linearly adsorbed CO (CO_L) on exposed Au sites is only 1/9 of that on bare Au film, suggesting a nearly full coverage of Pt on Au substrate. Notably, the νCO_L band and the bridge bonded CO band (νCO_B) on Au/Pt are redshifted by 19 cm^{-1} and blue-shifted by 21 cm^{-1}, respectively, as compared to those for Au/Pt-10 nm. Moreover, the $\nu CO_B/\nu CO_L$ band intensity ratio for the Au/Pt is significantly higher than that for the 3D-grown Pt-10 nm. These infrared spectra indicate not only partial electron transfer between Pt and Au but also a strengthened bonding of CO to Pt, which is consistent with the up-shift of the d-band center of Pt adlayer on Au[19, 20] owing to the lattice strain effect. Furthermore, our IR results also conform to those for the electrodeposited Pt ML on Au.[4] All the above results suggest the electroless method works well for the deposition of a q-ML of Pt on Au by using CO as the reducing and surface blocking reagents.

The feasible time for depositing a q-ML of Pt was assessed on an electrochemically cleaned Au disk electrode by monitoring the variation of OCP and the CV behaviour as shown in Fig. 2. The Au electrode was first immersed in 0.5 M $HClO_4$, and CO was kept bubbling in afterwards. After the OCP went steady, Pt(II) was added to reach a concentration of 0.1 mM. Within a few seconds, a sharp potential rise was observed. At the times indicated in Fig. 2(A) after adding Pt(II), the electrode was taken out, rinsed with Milli-Q water and served as the working electrode for Fig. 2(B). The CVs show that Pt coverage increases steadily from 1 to 10 min and largely stabilized afterwards, suggestive of the quenching effect of CO on newly formed Pt overlayer. As a result, Au/C was dispersed in the CO-saturated Pt(II)-bath for about 10 min.

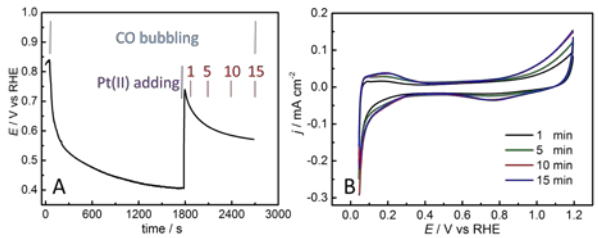

Fig. 2 (A) OCP vs time before and after Pt deposition onto Au electrode from CO-containing 0.5 M $HClO_4$. (B) CVs for the Au/Pt electrodes with varying Pt deposition time in 0.5 M $HClO_4$ at 50 mV s^{-1}.

High resolution TEM measurement on Au@Pt/C and Au/C does not reveal morphological change of Au nanoparticles (Fig. S3). X-ray diffractometry on Au/C, Au@Pt/C, Au@Pd/C and Au@(Pt+Pd)/C (Pt: Pd = 1: 2 in atomic ratio) reveals essentially same diffraction patterns without appreciable PGM peaks, which are consistent with a q-ML of PGM formed (Fig. S4). EDS elemental mapping indicates that most of Pt (Fig. 3) or Pd (Fig. S5) is distributed in the same area as Au, suggesting the preferential decomposition of PGM carbonyl complex on Au surfaces (Fig. S6). In addition, the central and edge parts of a randomly selected Au@Pt nanoparticle on carbon (Fig. 3B) exhibit the Au: Pt atomic ratio 1:0.16 and 1:0.87, respectively, suggestive of a core-shell structure instead of Pt-Au nanoalloy.

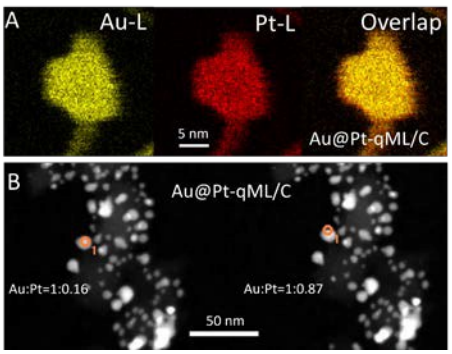

Fig. 3 (A) EDS elemental mapping images of a randomly selected Au@Pt-qML/C nanoparticle. (B) The center (left) and edge (right) parts of the nanoparticle for EDS measurement.

The feasible chemical deposition of PGM on Au is expected to find a wide application in (electro)-catalysis. As a preliminary investigation, alkaline ethanol oxidation reaction on commercial Pt/C, Pd/C and Au/C as well as on Au@Pt/C, Au@Pd/C and Au@(Pt+Pd)/C was examined by voltammetry. Fig. 4 shows CVs for EOR with current normalized by the total masses of Au and PGM. The onset potentials on Au@Pt/C, Au@Pd/C, Au@(Pt+Pd)/C or Pd/C in the forward scan are ca. 0.44, 0.44, 0.42 or 0.43 V, respectively, slightly negative of that on Pt/C (ca. 0.49 V) but far more negative than that on Au/C (ca. 0.82 V). Furthermore, the peak oxidation currents in the forward scan at ca. 0.85 V on Au@Pt/C, Au@Pd/C and Au@(Pt+Pd)/C are ca. 4.14, 2.28 and 8.99 A $mg^{-1}_{(Metal)}$, respectively, much higher than those on for Pt/C (ca. 0.63 A $mg^{-1}_{(Metal)}$) and Pd/C (ca. 1.70 A $mg^{-1}_{(Metal)}$). If only the masses of the PGMs are considered, the peak currents may reach 19.5, 13.7 and 45 A $mg^{-1}_{(PGM)}$ on Au@Pt/C, Au@Pd/C and Au@(Pt+Pd)/C,

respectively. Therefore, the Au substrate significantly boosts the EOR activity on Pt or Pd in alkaline media, which is in qualitatively agreement with that observed in acidic media.[5] Furthermore, the promoting effect of the underlying Au on EOR at Pt surface is much more pronounced in alkaline media than in acidic media (Fig. S7).

Notably, the separation of anodic peak potentials in the forward and backward scans on Au@Pt/C and Au@Pd/C is much smaller than that on Pt/C and Pd/C, respectively. This may arise from less formation of Pt (Pd) oxide when the potential was excursed to upper limit due to the electronic effect of underlying Au.[5] High-coverage oxide formation may severely deactivate a PGM catalyst in oxidizing ethanol. [21]

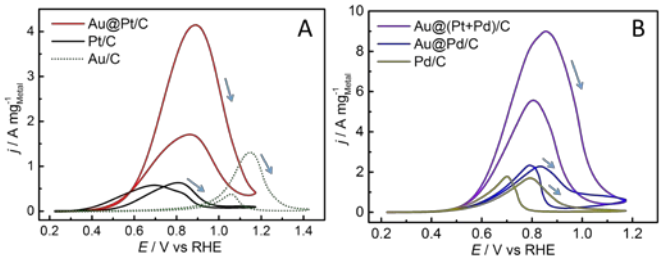

Fig. 4 Cyclic voltammograms of Au@Pt/C, Pt/C and Au/C (Left) and Au@(Pt+Pd)/C and Au@Pd/C (Right) in 1 M NaOH + 1 M C_2H_5OH solution at 50 mV s^{-1}.

Fig. 5 shows the chronoamperometric curves for the above catalysts in an alkaline ethanol solution at 0.75 V. At t = 60 min, the largest oxidation current was observed on Au@(Pt+Pd)/C and the smallest one on Pt/C. In addition, 16.3%, 21.3% and 15.1% of the initial oxidation currents remain on Au@Pt/C, Au@Pd/C and Au@(Pt+Pd)/C, respectively, but only 1.5% and 7.7% on Pt/C and Pd/C. The activity decay on an anode catalyst may come from the accumulated poisoning species as well as the decreasing interfacial concentration of reactants due to sustaining high oxidation currents. Obviously, the EOR current on Pt/C is much lower through the entire oxidation process, such a substantially decreased current is unlikely due to the latter effect.

As mentioned in the above, the Au@Pt and/or Pd structure may upshift the d-band center of the PGM shell,[19, 22] leading to a stronger adsorption of OH and ethanol. Further insight into the enhanced electrocatalysis of EOR in alkaline media on the as-synthesized Au@PGM/C is under investigation by combined spectro-electrochemistry and DFT calculation, and will be reported in due course.

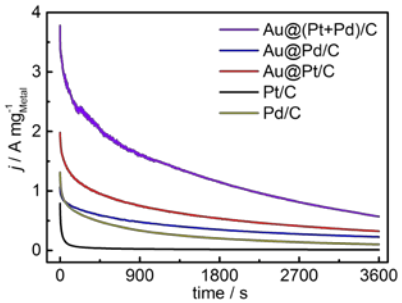

Fig. 5 Chronoamperometric curves for Au@Pt/C, Au@Pd/C, Au@(Pt+Pd)/C, Pt/C and Pd/C in 1 M NaOH + 1 M CH_3CH_2OH at 0.75 V vs RHE.

In addition, the CO-based chemical deposition can be used to qualitatively control Pt coverages by adjusting the deposition time and/or the precursor concentration. The effect of Pt-depostion time on the electrocatalytic activity and stability of Au@Pt/C in EOR is shown as preliminary results in Fig S8.

In summary, we have developed a facile electroless method that enables the controlled deposition of up to one monolayer of Pt and/or Pd on Au substrates in aqueous solution using CO as both reducing and quenching agents. This chemical protocol is suitable for scale-up synthesis of Au@PGM-based catalysts regardless of the forms of Au substrates and the supports. 14-fold enhancement in mass activity can be achieved on the Au@PGM/C as compared to that on the commercial Pt/C toward ethanol oxidation in alkaline media.

This work is supported by the 973 Program (No. 2015CB932303) of MOST, NSFC (Nos. 21473039 and 21273046).

Notes and references

†Shanghai Key Laboratory of Molecular Catalysis and Innovative Materials, Collaborative Innovation Center of Chemistry for Energy Materials, Department of Chemistry, Fudan University, Shanghai 200433, China;
E-mail: wbcai@fudan.edu.cn
‡State Key Laboratory of Physical Chemistry of Solid Surfaces, Collaborative Innovation Center of Chemistry for Energy Materials, Department of Chemistry, Xiamen University, Xiamen 361005, China

Electronic Supplementary Information (ESI) available. See DOI: 10.1039/c000000x/

1. T. Ralph and M. Hogarth, *Plat. Met. Rev.*, 2002, **46**, 117-135.
2. F. Vigier, S. Rousseau, C. Coutanceau, J.-M. Leger and C. Lamy, *Top. Catal.*, 2006, **40**, 111-121.
3. Y. H. Liu, D. Gokcen, U. Bertocci and T. P. Moffat, *Science*, 2012, **338**, 1327-1330.
4. S. Brimaud and R. J. Behm, *J. Am. Chem. Soc.*, 2013, **135**, 11716-11719.
5. M. Li, P. Liu and R. R. Adzic, *J. Phys. Chem. Lett.*, 2012, **3**, 3480-3485.
6. S. Cherevko, X. Xing and C.-H. Chung, *Electrochimi. Acta*, 2011, **56**, 5771-5775.
7. S. Cherevko, N. Kulyk and C.-H. Chung, *Electrochimi. Acta*, 2012, **69**, 190-196.
8. M. Shao, A. Peles, K. Shoemaker, M. Gummalla, P. N. Njoki, J. Luo and C.-J. Zhong, *J. Phys. Chem. Lett.*, 2011, **2**, 67-72.
9. N. Kristian, Y. Yan and X. Wang, *Chem Commun.*, 2008, 353-355.
10. G.-R. Zhang, D. Zhao, Y.-Y. Feng, B. Zhang, D. S. Su, G. Liu and B.-Q. Xu, *ACS Nano*, 2012, **6**, 2226-2236.
11. J.-F. Li, Z.-L. Yang, B. Ren, G.-K. Liu, P.-P. Fang, Y.-X. Jiang, D.-Y. Wu and Z.-Q. Tian, *Langmuir*, 2006, **22**, 10372-10379.
12. L. D. Zhu, T. S. Zhao, J. B. Xu and Z. X. Liang, *J. Power Sources*, 2009, **187**, 80-84.
13. Y. Dai and S. Chen, *ACS Appl. Mater. Interfaces*, 2014, **7**, 823-829.
14. H. F. Waibel, M. Kleinert, L. A. Kibler and D. M. Kolb, *Electrochimi. Acta*, 2002, **47**, 1461-1467.
15. S. Brankovic, J. Wang and R. Adzic, *Surf. Sci.*, 2001, **474**, L173-L179.
16. R. Loukrakpam, Q. Yuan, V. Petkov, L. Gan, S. Rudi, R. Yang, Y. Huang, S. R. Brankovic and P. Strasser, *Phys. Chem. Chem. Phys.*, 2014, **16**, 18866-18876.
17. J. Kim, J. Lee, S. Kim, Y.-R. Kim and C. K. Rhee, *J. Phys. Chem. C*, 2014, **118**, 24425-24436.
18. R. E. Benfield, *J. Chem. Soc., Faraday Trans.*, 1992, **88**, 1107-1110.
19. E. Casado-Rivera, D. J. Volpe, L. Alden, C. Lind, C. Downie, T. Vazquez-Alvarez, A. C. D. Angelo, F. J. DiSalvo and H. D. Abruna, *J. Am. Chem. Soc.*, 2004, **126**, 4043-4049.
20. B. Hammer and J. K. Norskov, *Adv. Catal.*, 2000, **45**, 71-129.
21. L. Wang, A. Lavacchi, M. Bevilacqua, M. Bellini, P. Fornasiero, J. Filippi, M. Innocenti, A. Marchionni, H. A. Miller and F. Vizza, *ChemCatChem*, 2015, **7**, 2214-2221.
22. B. Hammer and J. K. Norskov, *Nature*, 1995, **376**, 238-240.